Materials Science in Semiconductor Processing 15 (2012) 432–437

Contents lists available at SciVerse ScienceDirect

Materials Science in Semiconductor Processing

journal homepage: www.elsevier.com/locate/mssp

Substrate temperature effect on structural, optical and electrical properties of vacuum evaporated SnO_2 thin films

Mehdi Zadsar [a,*], Hamid Reza Fallah [a,b], Morteza Haji Mahmoodzadeh [a,b], Ali Hassanzadeh [c], Mohsen Ghasemi Varnamkhasti [a]

[a] Department of Physics, University of Isfahan, Isfahan, Iran
[b] Quantum Optics Research Group, University of Isfahan, Isfahan, Iran
[c] Department of Chemistry, University of Urmia, Urmia, Iran

ARTICLE INFO

Available online 9 March 2012

Keywords:
Tin oxide films
Transparent conductive oxide
Substrate temperature
Optical transmission
Electrical properties

ABSTRACT

Tin oxide (SnO_2) thin films were deposited on glass substrates by thermal evaporation at different substrate temperatures. Increasing substrate temperature (T_s) from 250 to 450 °C reduced resistivity of SnO_2 thin films from 18×10^{-4} to 4×10^{-4} Ω cm. Further increase of temperature up to 550 °C had no effect on the resistivity. For films prepared at 450 °C, high transparency (91.5%) over the visible wavelength region of spectrum was obtained. Refractive index and porosity of the layers were also calculated. A direct band gap at different substrate temperatures is in the range of 3.55 – 3.77 eV. X-ray diffraction (XRD) results suggested that all films were amorphous in structure at lower substrate temperatures, while crystalline SnO_2 films were obtained at higher temperatures. Scanning electron microscopy images showed that the grain size and crystallinity of films depend on the substrate temperature. SnO_2 films prepared at 550 °C have a very smooth surface with an RMS roughness of 0.38 nm.

1. Introduction

Tin oxide (SnO_2) is a non-stoichiometric semiconductor with a wide band gap ($E_g \geq 3.1$ eV) at room temperature with tetragonal structure [1]. SnO_2 films have unique characteristics such as low cost, low resistivity, high transmittance in visible wavelength region, and high chemical and thermal stabilities compared to other transparent conductive oxides (TCOs) [2]. SnO_2 films are widely used in optoelectronic applications, heat mirror coatings, photocatalysis, organic light emitting diodes, gas sensors, solar energy collectors and so on [3–8]. There are several methods for preparing SnO_2 films: spray pyrolysis [9], chemical vapor deposition [10], electron beam evaporation [11], reactive sputtering [12], metal–organic deposition [13], sol–gel deposition [14] and thermal evaporation [15]. Among these methods, thermal evaporation has the advantages of producing high purity crystalline products and durable films in a single step. Various parameters such as annealing temperature, deposition rate, oxygen partial pressure and substrate temperature have significant influence on characteristics of SnO_2 films. Among these parameters, substrate temperature has a major role in decreasing the intrinsic stress, increasing mobility of charge carriers, and improving homogeneity and crystallinity of films to get better quality films. To the best of our knowledge, not much attention has been paid to the study of the substrate temperature effect on characteristics of non-doped SnO_2 thin films deposited by thermal evaporation in literature. Since the thermal evaporation is

* Corresponding author. Tel.: +98 311 7932428; fax: +98 311 7932435.
E-mail addresses: mphdzadsar@gmail.com (M. Zadsar), hrf64@yahoo.com (H.R. Fallah), morteza16@yahoo.com (M. Haji Mahmoodzadeh), Ali.hassanzadeh@gmail.com (A. Hassanzadeh), m_gh_v@yahoo.com (M. Ghasemi Varnamkhasti).

1369-8001/$ - see front matter © 2012 Elsevier Ltd. All rights reserved.
doi:10.1016/j.mssp.2012.02.011

not a conventional technique to deposit non-doped SnO_2 films, it seems that this work would be of interest for researchers.

In this work, the structural, optical and electrical properties of SnO_2 thin films deposited on glass substrates at various deposition temperatures by thermal evaporation have been investigated using X-ray diffraction (XRD), scanning electron microscopy (SEM), atomic force microscopy (AFM), UV–visible spectrophotometer and a conventional four point probe technique.

2. Experimental procedure

SnO_2 films were deposited on glass substrate by thermal evaporation. The distance between the substrate and the target was 12 cm and substrate temperature was varied between 250 and 550 °C to investigate the influence of substrate temperature on structural, electrical and optical properties. The working pressure was kept below 3×10^{-5} mbar. The source for evaporation in our method was a 99.99% pure SnO_2 powder. Before deposition, glass substrates were first rinsed in acetone, isopropyl alcohol and ethanol, with ultrasonic vibration for 10 minutes. The substrates were dried at 120 °C for 1 h in the furnace after rinsing with deionized water. Deposition rate was fixed at 0.1 nm s^{-1}. The film thickness was measured using a quartz crystal thickness monitor and was kept at 400 nm for all samples. The microstructure of the SnO_2 films was examined by X-ray diffraction measurements (D8 Advance Bruker X-ray diffractometer with a 10 kV, 35 mA, Cu Kα radiation with wavelength of 1.548 Å) and scanning electron microscopy (SEM). The surface morphology was also performed using an atomic force microscope (AFM, Model DS-95-200E). The resistivity of thin films was characterized by a four point probe method. A double-beam spectrophotometer (Shimadzu UV 3100) was used to measure optical transmittance of SnO_2 films.

3. Results and discussion

3.1. Structural properties

Fig. 1 shows the XRD patterns of the SnO_2 thin films at substrate temperature from 250 to 550 °C for 2θ scans between 10° and 70°. It can be found that films deposited at 250 °C were nearly amorphous whereas for higher temperatures, the amorphous background was diminished and diffraction peak (110) of standard SnO_2 powder revealed for all samples as mentioned by other researchers [16]. The peak intensity and sharpness increased with increasing substrate temperature. This confirms that crystallinity of the films improves with increasing substrate temperature and it can be expected that these films are composed of nanoparticles. In order to determine the influence of substrate temperature on crystallite size of SnO_2 films, size of the crystallites oriented along (110) plane is estimated by Scherrer's formula [17]

$$D = 0.9\lambda/\beta\cos\theta \quad (1)$$

where D is the grain size, λ (1.548 Å) is the wavelength of X-ray radiation, β is the full width at half maximum

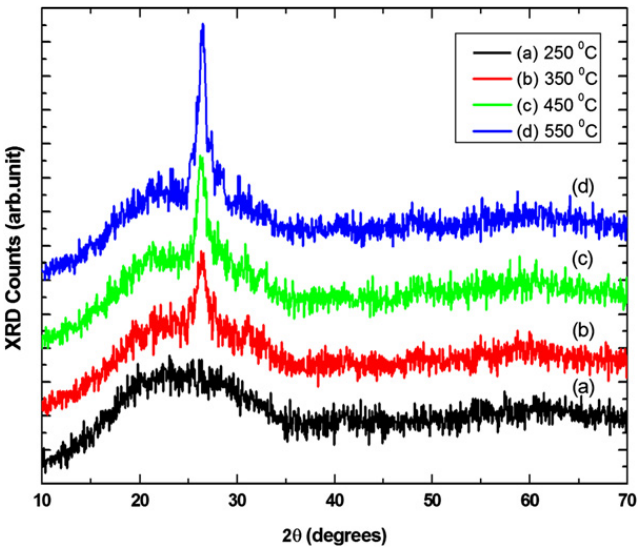

Fig. 1. XRD patterns of the SnO_2 films fabricated at various substrate temperatures.

(FWHM) of the diffraction peak and θ is the Bragg diffraction angle of the XRD peak. Table 1 shows the evolution of average crystallite size according to the substrate temperature. It can be seen that substrate temperature has an effective influence on the crystallite size, which increases from 25.2 to 79.9 nm. The increase of crystallite size is due to the fact that the substrate temperatures higher than 250 °C during deposition are usually relatively high enough to provide sufficient thermal energy for recrystallization. Hence, crystallization process improved and the smaller crystallites agglomerated with increasing substrate temperature to cause a change in crystallite size distribution towards larger crystallites. This result is in agreement with those of other researchers [18].

In order to study surface topography changes of SnO_2 films deposited at different substrate temperatures, scanning electron microscopy (SEM) was used. Fig. 2(a), (b), (c) and (d) shows the SEM images of the films deposited at 250, 350, 450 and 550 °C respectively. It can be seen that the grain size becomes larger with increasing substrate temperature which agrees with afore-mentioned results of the XRD analysis. Generally, surface thermal energy has influences on crystallite size and morphology of the films. The amorphous structure of SnO_2 films deposited at lower deposition temperature (250 °C) is related to relatively lower thermal energy. However at higher temperatures, nucleation and growth process alters and the grain size grows.

It is known that the structural and surface morphological properties of SnO_2 films as TCOs can affect the electrical and optical characteristics of devices based on these films [19]. For example, in the electro-optical devices such as flat panel displays and light emitting diodes, surface roughness of SnO_2 films as transparent electrodes has direct implication for determining and improving the device performance and life time [6]. Therefore, it is very important to examine the surface morphological properties of SnO_2 films. Two-dimensional

Table 1
Crystallite size, RMS roughness, refractive index, porosity and Band-gap energy of SnO_2 films with different substrate temperatures (Films thickness is 400 nm).

Substrate temperature (°C)	Crystallite size (nm)	RMS roughness (nm)	Refractive index at 550 nm	Porosity (%)	Band gap energy (eV)
250	–	4.1 ± 0.01	2.03	7.30	3.77 ± 0.02
350	25.2 ± 0.3	2.2 ± 0.01	2.04	6.13	3.65 ± 0.02
450	70.3 ± 0.4	0.8 ± 0.01	1.77	36.6	3.57 ± 0.02
550	79.9 ± 0.5	0.38 ± 0.01	1.85	28.0	3.55 ± 0.02

Experimental errors in temperature $\Delta T = \pm 1$ °C

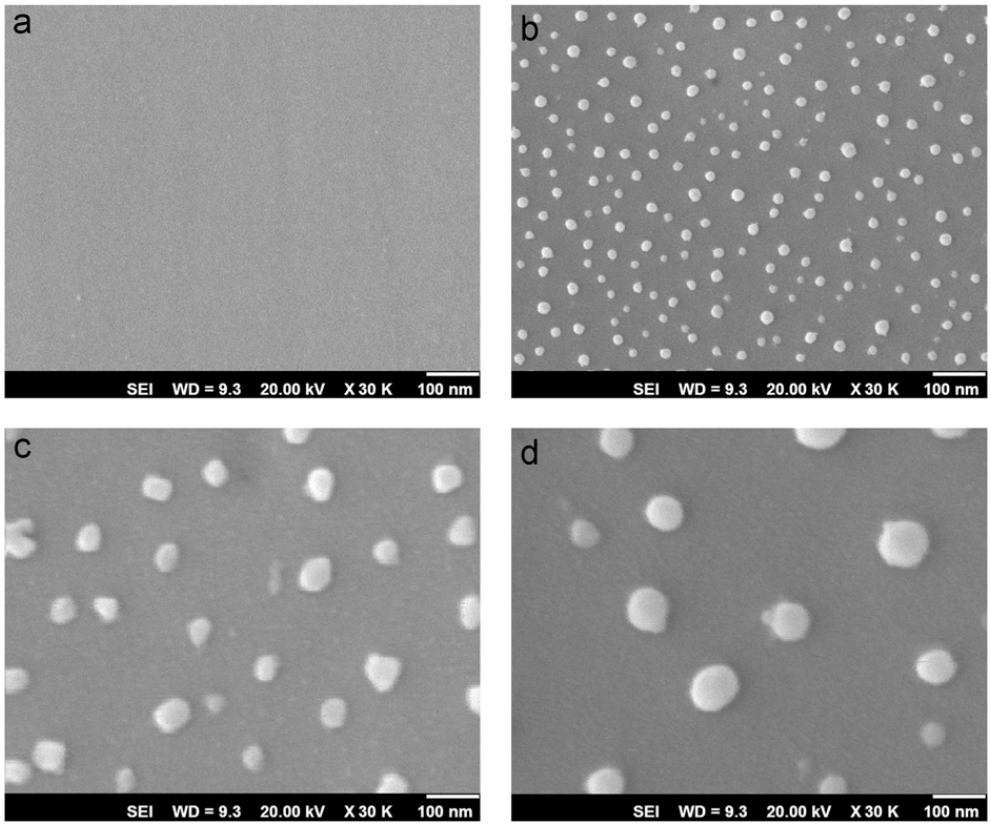

Fig. 2. SEM images of the SnO_2 films at different substrate temperatures: (a) 250 °C, (b) 350 °C, (c) 450 °C and (d) 550 °C.

AFM images of the SnO_2 films prepared at different substrate temperatures shown in Fig. 3(a)–(d) were measured in a dynamic mode over a 5 μm × 5 μm area of the film surface. The 2D images of SnO_2 thin films clearly indicate that grain size increases with increasing substrate temperature and the SnO_2 thin film prepared at 550 ºC has particles of larger size compared to other films. This also confirms SEM results. The root-mean-square (RMS) roughnesses of SnO_2 films prepared at different substrate temperatures are provided in Table 1. It is observed that the surface roughness of the SnO_2 films is sensitive to the substrate temperature and the RMS roughness of films decreases with increasing substrate temperature. In fact, smoother films can be obtained at higher substrate temperature. When the substrate temperature increases, surface thermal energy of samples enhances and the grains grow in a continuous and uniform structure. Consequently, the RMS roughness of SnO_2 films decreases and its minimum value is obtained for the sample prepared at 550 ºC.

3.2. Electrical properties

Fig. 4 shows a plot of resistivity as a function of substrate temperature for SnO_2 films. It was observed that resistivity in the temperature range of 250–550 °C decreases from 18×10^{-4} to $4 \times 10^{-4}\,\Omega\,cm$ with the substrate temperature up to 450 °C and was fixed thereafter. The obtained values of resistivity in this work are lower than those of sprayed tin oxide thin films [20,21]. It is well known that the conductivity of TCO thin films is influenced by different scattering processes [22]. The main scattering mechanisms in these structures are the impurities and grain boundaries. Since SnO_2 thin films are deposited in high vacuum, the high-purity films can be fabricated on glass substrates. Thus, it seems that grain boundaries are the dominant scattering mechanisms in SnO_2 films. In the temperature range of 250–450 ºC, as the crystallite size grows and the orientation of the grain changes, grain boundaries narrow, scattering of charge carriers decreases and thus mobility of charge

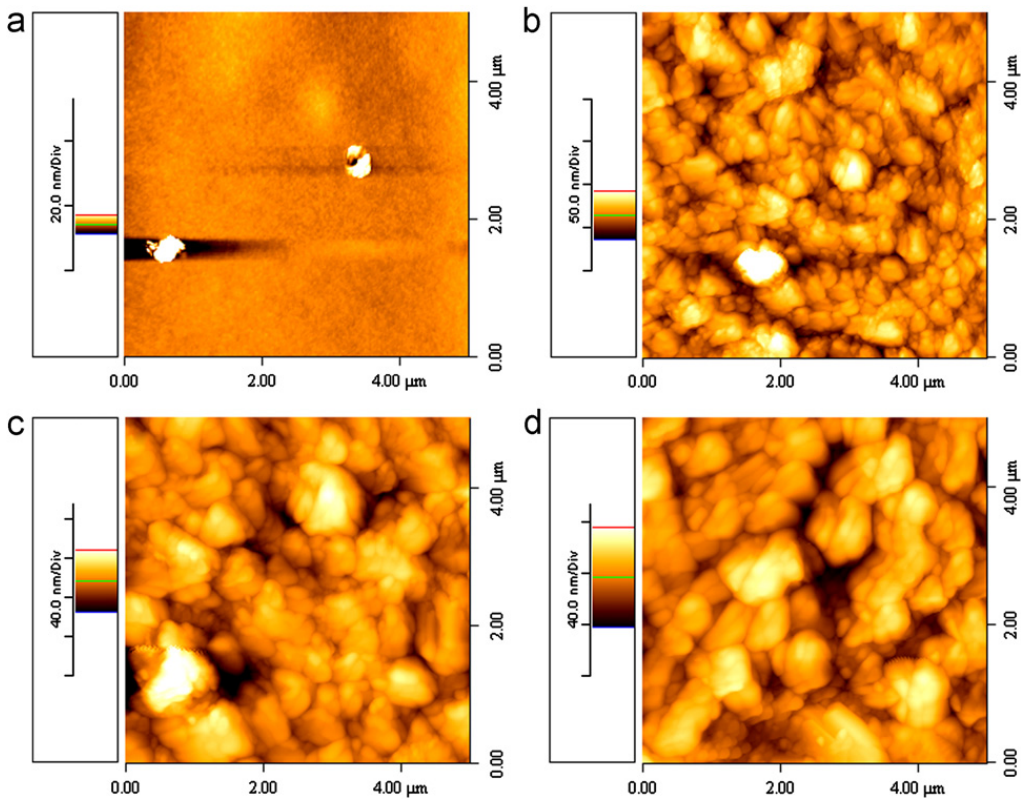

Fig. 3. Two-dimensional AFM images of the SnO_2 films at different substrate temperatures: (a) 250 °C, (b) 350 °C, (c) 450 °C and (d) 550 °C.

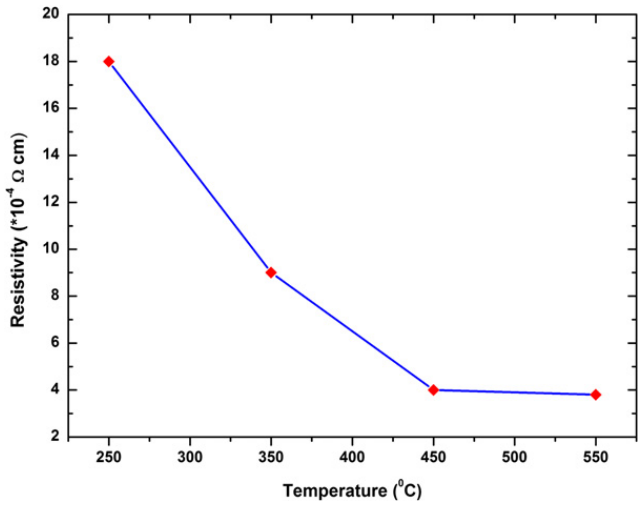

Fig. 4. Resistivity of the SnO_2 films as a function of substrate temperature.

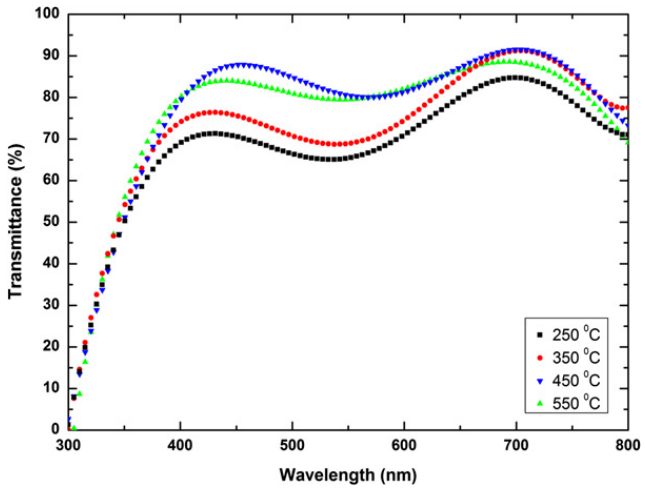

Fig. 5. Optical transmission spectra of the SnO_2 films at the various substrate temperatures.

carriers increases. As a consequence, it is expected that the resistivity decreases. This is also confirmed from the AFM results. As the substrate temperature increases and the film surface smoothens, the uniformity and morphology of SnO_2 films improve, which results in the increase of the flow of electrons and so the resistivity decreases. However, with further increase of substrate temperature, the crystal growth process is completed and no more increase in crystallite size occurs, so decrease in resistivity becomes saturated and it approaches a constant value.

3.3. Optical transmittance

Fig. 5 shows the optical transmittance spectrum of SnO_2 films in the region of 300–800 nm for different substrate temperatures. It is clear that the optical transmission of these films varies over the range of 65–91.5%. An increase in transmittance with substrate temperature is clearly observed for $\lambda < 600$ nm. This increase in transmittance is due to the increase in the crystallinity of films after annealing which results in lower scattering of light. This result agrees with the discussion of the structural analysis of films. The ripples

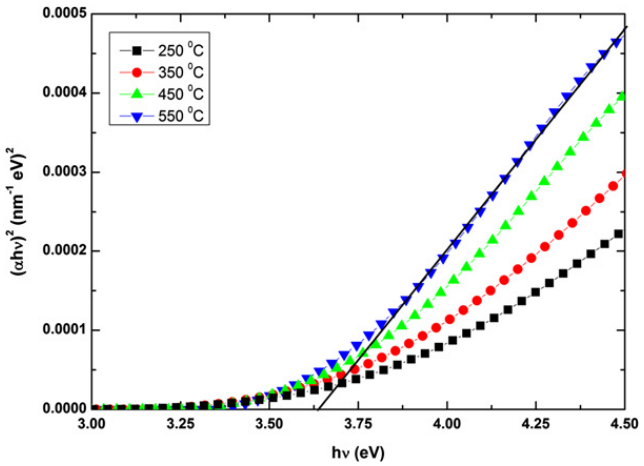

Fig. 6. Band-gap (E_g) estimation of SnO_2 films from Tauc relation.

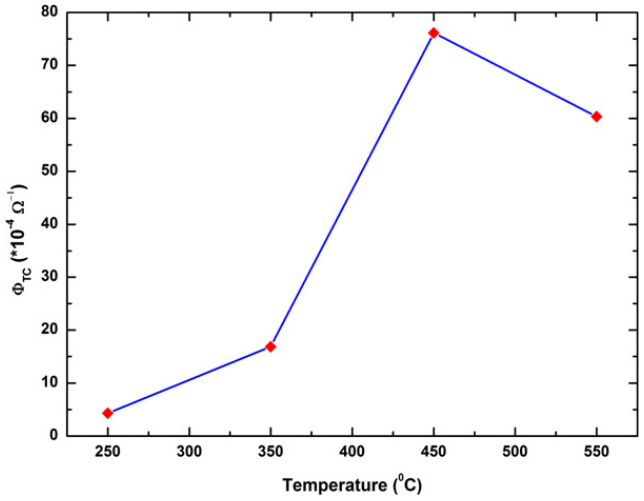

Fig. 7. The figure of merit (Φ_{TC}) values of the SnO_2 films as a function of substrate temperature.

in transmission spectra are attributed to optical interference effects. The refractive index of the deposited SnO_2 films was estimated from the measured transmittance spectra using envelops method [23]. In this method the refractive index can be calculated by these formulas:

$$n(\lambda)=\sqrt{S+\sqrt{S^2-n_0^2\,(\lambda)\,n_s^2\,(\lambda)}} \tag{2}$$

$$S=\frac{1}{2}(n_0^2\,(\lambda)+n_s^2\,(\lambda))+2n_0n_s\left(\frac{T_{max}(\lambda)-T_{min}(\lambda)}{T_{max}(\lambda)T_{min}(\lambda)}\right) \tag{3}$$

where n_0 is the refractive index of air, n_s is the refractive index of substrate, T_{max} is the maximum envelope, and T_{min} is the minimum envelope. Also, the porosity of the SnO_2 films was calculated using the following equation [24]:

$$Porosity=\left(1-\frac{n^2-1}{n_d^2-1}\right)\times 100\,(\%) \tag{4}$$

where n_d is the refractive index of pore-free SnO_2 and n is the refractive index of the porous thin films. The refractive index (n) and the porosity of SnO_2 films were listed as a function of substrate temperature in Table 1. As can be seen, the refractive index of these films (at $\lambda=550$ nm) decreases with increasing substrate temperature from 2.04 to 1.77. The decrease of refractive index in SnO_2 thin films can be ascribed to the increasing porosity. For the porosity, a maximum value (36.6%) was obtained for SnO_2 thin film grown at 450 ºC.

3.4. Estimation of the band gap

Ignoring the reflectivity which is expected to be low, the absorption coefficient has been obtained from the Lambert's formula, as follows:

$$\alpha=\frac{\ln(1/T)}{d} \tag{5}$$

where, d and T are the film thickness and transmittance, respectively. According to the literatures, the band gap of SnO_2 films is a direct transition in nature [25]. The absorption coefficient (α) is a function of photon energy for direct transitions that can be written as

$$\alpha h\upsilon=A(h\upsilon-E_g)^{1/2} \tag{6}$$

where A is an energy-independent constant and E_g is the optical band gap. In order to estimate the band gap energy of the SnO_2 films, the plots of $(\alpha h\upsilon)^2$ versus $h\upsilon$ are drawn in Fig. 6. The direct band gap is obtained by extrapolating the straight portion of this curve to zero absorption ($\alpha=0$). The direct band-gap values of SnO_2 films are given in Table 1 for different substrate temperatures. The obtained energy gap values are in good agreement with other literature reports [26]. It is found that the band gap energy decreases with increasing substrate temperature up to 450 °C and then it varies only slightly with further increase in temperature. The values of band gap lie in the range of 3.55–3.77 eV. This result can be attributed to the decrease of grain boundaries as scattering centers. In fact, the increase of substrate temperature improves crystallinity and increases average crystallite size which results in decreasing grain boundaries; therefore band gap energy decreases.

The figure of merit (Φ_{TC}) is an useful parameter for comparing the performance of transparent conductive oxide (TCO) films that was defined by Haacke [27] as

$$\Phi_{TC}=\frac{T^{10}}{R_s} \tag{7}$$

where T is the average transmission and R_s is the sheet resistance. The calculated value of figure of merit (Φ_{TC}) as a function of substrate temperature is shown in Fig. 7. It can be seen that the deposited films at 450 °C have higher Φ_{TC} ($76.12\times10^{-4}\ \Omega^{-1}$) than other films. Thus, this film can be used as an optimum transparent conductive electrode for optoelectronics applications.

4. Conclusion

SnO_2 films were deposited by thermal evaporation at various substrate temperatures in the range of 250–550 °C. The XRD patterns and the SEM images showed that the crystallinity in non-doped SnO_2 films improved and grain size became larger with increasing substrate

temperature. Also, AFM analysis indicated that the RMS roughness of films decreased with substrate temperature and the sample prepared at 550 ọC showed the minimum value of RMS roughness compared to other samples. The resistivity of the films was decreased with increase of substrate temperature up to 450 °C and was fixed thereafter. It was observed that the optical transparency of non-doped SnO_2 can be affected by substrate temperature. Films deposited at 450 °C have the highest Φ_{TC} ($76.12\times10^{-4}\,\Omega^{-1}$). Finally, substrate temperature has a major role in controlling optoelectrical properties.

Acknowledgment

The authors wish to thank the graduate office of the University of Isfahan for their support. Also, they are greatly indebted to the Iran Nanotechnology Initiative Council for their financial support.

References

[1] The Joint Committee on Powder Diffraction Standards (JCPDS), Card No. 77-0452, International Centre for Diffraction Data (ICDD), Swarthmore, PA, USA, 1978.
[2] B. Thangaraju, Thin Solid Films 402 (2002) 71–78.
[3] I.H. Kim, J.H. Ko, D. Kim, K.S. Lee, T.S. Lee, J.-h. Jeong, et al., Thin Solid Films 515 (2006) 2475–2480.
[4] Y.M. Lu, C.P. Hu, Journal of Alloys and Compounds 449 (2008) 389–392.
[5] S.S. Srinivasan, J. Wade, E.K. Stefanakos, Y. Goswami, Journal of Alloys and Compounds 424 (2006) 322–326.
[6] D. Vaufrey, M. Ben Khalifa, M.P. Besland, C. Sandu, M.G. Blanchin, V. Teodorescu, et al., Synthetic Metals 127 (2002) 207–211.
[7] M.R. Yang, S.Y. Chu, R.C. Chang, Sensors and Actuators B 122 (2007) 269–273.
[8] S. Peng, F. Cheng, J. Liang, Z. Tao, J. Chen, Journal of Alloys and Compounds 481 (2009) 786–791.
[9] D. Paul Joseph, P. Renugambal, M. Saravanan, S. Philip Raja, C. Venkateswaran, Thin Solid Films 517 (2009) 6129–6136.
[10] F. Yu, D. Tang, K. Hai, Zh. Luo, Y. Chen, X. He, et al., Journal of Crystal Growth 312 (2010) 220–225.
[11] A.F. Khan, M. Mehmood, M. Aslam, M. Ashraf, Applied Surface Science 256 (2010) 2252–2258.
[12] M.A. Gubbins, V. Casey, S.B. Newcomb, Thin Solid Films 405 (2002) 270–275.
[13] T. Tsuchiya, K. Daoudi, I. Yamaguchi, T. Manabe, T. Kumagai, S. Mizuta, Applied Surface Science 247 (2005) 145–150.
[14] W. Hamd, Y.C. Wu, A. Boulle, E. Thune, R. Guinebretière, Thin Solid Films 518 (2009) 1–5.
[15] N.M. Shaalan, T. Yamazaki, T. Kikuta, Sensors and Actuators B: Chemical 153 (2011) 11–16.
[16] D. Miao, Q. Zhao, Sh. Wu, Zh. Wang, X. Zhang, X. Zhao, Journal of Non-Crystalline Solids 356 (2010) 2557–2561.
[17] E. Gagaoudakis, M. Bender, E. Douloufakis, N. Katsarakis, E. Natasakou, V. Cimalla, et al., Sensors and Actuators B 80 (2001) 155–161.
[18] P.S. Patil, R.K. Kawar, T. Seth, D.P. Amalnerkar, P.S. Chigare, Ceramics International 29 (2003) 725–734.
[19] Z. Remes, M. Vanecek, H.M. Yates, P. Evans, D.W. Sheel, Thin Solid Films 517 (2009) 6287–6289.
[20] V. Vasu, A. Subrahmanyam, Thin Solid Films 189 (1990) 217–225.
[21] R.R. Kasar, N.G. Deshpande, Y.G. Gudage, J.C. Vyas, R. Sharma, Physica B 403 (2008) 3724–3729.
[22] A.V. Moholkar, S.M. Pawar, K.Y. Rajpure, C.H. Bhosale, Journal of Alloys and Compounds 455 (2008) 440.
[23] J.C. Manifacier, J. Gasiot, J.P. Fillard, Journal of Physics E 9 (1976) 1002–1004.
[24] S.H. Oh, D.J. Kim, S.H. Hahn, E.J. Kim, Materials Letters 57 (2003) 4151–4155.
[25] K.L. Chopra, S. Major, D.K. Pandya, Thin Solid Films 102 (1983) 1–46.
[26] T. Serin, N. Serin, S. Karadeniz, H. Sarı, N. Tuğluoğlu, O. Pakma, Journal of Non-Crystalline Solids 352 (2006) 209–215.
[27] G. Haacke, Journal of Applied Physics 47 (1976) 4086–4089.